



Cite this: DOI: 10.1039/c8dt04116d

Synthesis and characterisation of homoleptic 2,9-diaryl-1,10-phenanthroline copper(i) complexes: influencing selectivity in photoredox-catalysed atom-transfer radical addition reactions†

Thomas P. Nicholls,^a Chiara Caporale,^{id b} Massimiliano Massi,^{id b} Michael G. Gardiner^{id a} and Alex C. Bissember^{id *a}

This report details the synthesis and characterisation of eight homoleptic bis(2,9-diaryl-1,10-phenanthroline)copper(i) complexes, seven of which are previously unreported {aryl = *p*-CF₃C₆H₄, *p*-FC₆H₄, *m,p*-(OMe)₂C₆H₃, *o,p*-(OMe)₂C₆H₃, *p*-OMe-*m,m*-Me₂C₆H₂, *p*-OMe-*m,m*-(*t*-Bu)₂C₆H₂, 9,9-dimethyl-9*H*-fluoren-2-yl, 4-(9*H*-carbazol-9-yl)phenyl}. Where possible the solid state, photophysical and electrochemical properties of these complexes were studied. In order to obtain insights into the influence of the intrinsic features of these copper(i) complexes on their reactivity in visible light-mediated photoredox catalysis, their capacity to promote a known atom-transfer radical addition process was evaluated. This specific transformation was identified as a suitable model system as it is reported to proceed *via* a mechanism consistent with the inner-sphere reactivity enabled by coordinatively unsaturated phenanthroline-based copper(i) species.

Received 15th October 2018,
Accepted 13th February 2019

DOI: 10.1039/c8dt04116d

rsc.li/dalton

Introduction

In comparison to ubiquitous photoredox catalysts featuring second- or third-row transition metals, such as [Ru(bpy)₃]Cl₂ (2), copper-based photoredox catalysts, including [Cu(dap)₂]Cl (1-Cl), have received much less attention in photoredox catalysis (Fig. 1).^{1,2} The distinctive feature of copper(i) complexes is their preference for the metal centre to adopt a tetrahedral coordination geometry. However, upon photoexcitation to the metal-to-ligand-charge transfer (MLCT) manifold, the temporary formation of a copper(ii) ion favours distortion of the metal centre from tetrahedral to square planar coordination geometries.³ In addition to reducing the coordinative stability of these complexes and potentially favouring the coordination of a solvent molecule or counteranion, this structural reorganisation is known to offer facile non-radiative pathways from the excited states *via* enhancement of the non-radiative decay constant *k*_{nr}, with consequent reduction of the excited state lifetime and quantum yield values.^{1b} Perhaps, in part, because of

these challenges, examples of synthetic reactions employing phenanthroline-based visible light-mediated copper(i) photoredox catalysts are not as well established as those utilising coordinatively saturated, octahedral ruthenium and iridium systems.^{4–6}

We were interested in preparing a series of novel homoleptic phenanthroline containing copper(i) complexes featuring sterically- and electronically-varied 2,9-diaryl-1,10-phenanthroline ligands in order to improve our understanding of the influence of substituent effects on the photoredox capacity.⁷ With this in mind, we evaluated the viability of these novel homoleptic (in addition to known homoleptic and heteroleptic) copper(i) photoredox catalysts in a notable atom-transfer radical addition (ATRA) reaction that was recently reported (Scheme 1).^{5f} We specifically selected this model system as the

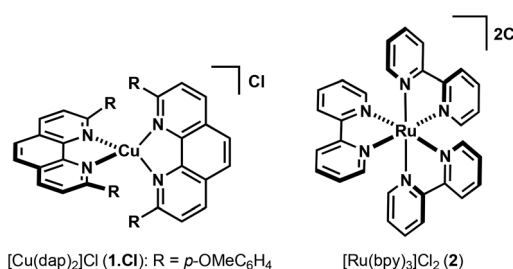
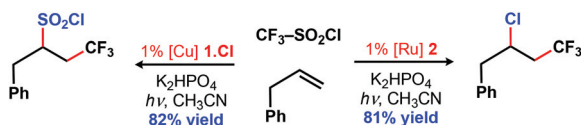


Fig. 1 Examples of established photoredox catalysts.

^aSchool of Natural Sciences – Chemistry, University of Tasmania, Hobart, Tasmania, 7001, Australia. E-mail: alex.bissember@utas.edu.au

^bDepartment of Chemistry and Nanochemistry Research Institute, Curtin University, Bentley, Western Australia, 6102, Australia

† Electronic supplementary information (ESI) available. CCDC 1872365–1872368. For ESI and crystallographic data in CIF or other electronic format see DOI: 10.1039/c8dt04116d



Scheme 1 Divergent reactivity provided by $[\text{Cu}(\text{dap})_2]\text{Cl}$ (**1-Cl**) in ATRA transformations identified by Reiser and co-workers.^{5f}

mechanism responsible for this transformation is consistent with the unusual inner-sphere reactivity provided by coordinatively unsaturated copper(i) photoredox catalysts, such as $[\text{Cu}(\text{dap})_2]\text{Cl}$ (**1-Cl**).^{5f,k,l,n,o} Consequently, we anticipated that this intriguing ATRA process, which has only been mediated by photoactive copper(i) species,^{5f,k,l} would allow us to indirectly study the influence of the structural features and other fundamental properties of these copper(i) catalysts on controlling the reaction outcome.

Herein, we report the synthesis, characterisation, and photocatalytic studies of the homoleptic bis(2,9-diaryl-1,10-phenanthroline)copper(i) complexes **3a–h**, seven of which are previously unreported (Fig. 2). Due to the presence of the π -conjugated coordinating ligands, all these complexes can be excited to MLCT excited states, as evidenced from the UV-Vis absorption spectra. The solid state structures of three of these complexes were determined by X-ray crystal structure analyses. Each of the complexes **1-PF₆**, **3a**, **3f** and **3g** display distorted tetrahedral coordination geometries about the metal centres and overall structure of the complex ions and the extent of this distortion has been quantified by examination of flattening, rocking and wagging distortions. The steric bulk of 2,9-diaryl substituents play a significant role in the extent of the distortion in the complexes in the ground state. These homoleptic copper(i) species, and various known heteroleptic copper(i) complexes, were evaluated in order to determine their capacity to promote ATRA processes of the type illustrated in Scheme 1. The relative ratios of trifluoromethylchlorosulfonation and trifluoromethylchlorination products in these photoredox-catalysed reactions were generally consistent with the varying steric bulk of the copper complex employed. However, electronic effects were also found to be important.

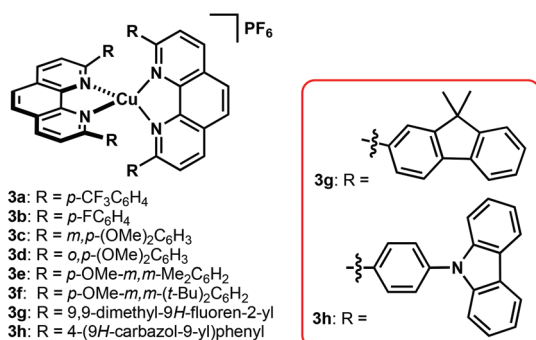


Fig. 2 Homoleptic copper(i) complexes synthesised in this study.

Experimental

Materials and methods

Anhydrous CH₂Cl₂ was distilled over CaH₂, under N₂, and stored over molecular sieves, under N₂, prior to use. PhMe and CH₃CN were purchased from Chem-Supply and passed through columns on an Innovative Technologies Solvent Purification system. 2,9-Dichloro-1,10-phenanthroline (**4**),⁸ $[\text{Cu}(\text{dap})_2]\text{Cl}$ (**1-Cl**),^{5a} $[\text{Cu}(\text{dmp})_2]\text{Cl}$ ⁹ (dmp = 2,9-dimethyl-1,10-phenanthroline), heteroleptic complexes **12a–d**,¹⁰ and compounds **10** and **11**,^{5f} were prepared *via* literature procedures. $[\text{Cu}(\text{CH}_3\text{CN})_4]\text{PF}_6$ and CF₃SO₂Cl were purchased from Sigma-Aldrich and used as received. Unless otherwise noted, all other starting materials were either purchased from commercial sources and used as received or prepared according to reported procedures. NMR experiments were performed either on a Bruker Avance III NMR spectrometer operating at 400 MHz (¹H), 100 MHz (¹³C), or 376 MHz (¹⁹F) or on a Bruker Avance III NMR spectrometer operating at 600 MHz (¹H), 150 MHz (¹³C), or 576 MHz (¹⁹F). The deuterated solvent used was CDCl₃, CD₃CN or DMSO-*d*₆. Our custom photoreactor was constructed using a strip of blue LEDs purchased from aliexpress.com. This photoreactor operated at 24 W (12 V, 2 A) to provide light predominantly at 467 nm.

Synthesis of ligands

General procedure 1. Ligands **5a,c–g** were synthesised by modifying conditions previously reported by Sauvage and co-workers.¹¹ These reactions were unoptimised. A solution of Na₂CO₃ (18 equiv.) in H₂O was added to a magnetically stirred solution of 2,9-dichloro-1,10-phenanthroline (**4**) (1 equiv.) and the organoborane (4 equiv.) in PhMe maintained at ambient temperature under N₂. $[\text{Pd}(\text{PPh}_3)_4]$ (10%) was added and the ensuing mixture was heated at 95 °C. After 16 h, the mixture was cooled to ambient temperature, the phases separated, and the aqueous phase was extracted with CH₂Cl₂ (2 × 20 mL). The combined organic extracts were then dried (Na₂SO₄), filtered, and concentrated under reduced pressure. The ensuing residue was purified by flash column chromatography on silica gel.

General procedure 2. Ligands **5b** and **5h** were synthesised by modifying conditions previously reported by Stille and co-workers.¹² These reactions were unoptimised. $[\text{Pd}(\text{PPh}_3)_4]$ (5%) was added to a magnetically stirred solution of the organostannane (4 equiv.) and 2,9-dichloro-1,10-phenanthroline (**4**) (1 equiv.) in PhMe maintained at ambient temperature under N₂. The ensuing mixture was heated to 110 °C. After 20 h, the mixture was cooled to ambient temperature and concentrated under reduced pressure. The ensuing residue was purified by flash column chromatography on silica gel.

2,9-Di(4-(trifluoromethyl)phenyl)-1,10-phenanthroline (5a). Reaction with 4-(trifluoromethyl)phenylboronic acid (610 mg, 3.21 mmol) following General procedure 1 and purified by flash column chromatography on silica gel (0–20% EtOAc/hexanes to provide compound **5a** as a colourless amorphous solid (182 mg, 48% yield). ¹H NMR (400 MHz, CDCl₃): δ 8.57

(d, $J = 8.5$ Hz, 4H), 8.39 (d, $J = 8.5$ Hz, 2H), 8.20 (d, $J = 8.5$ Hz, 2H), 7.90–7.86 (complex m, 6H) ppm. ^{13}C NMR (100 MHz, CDCl_3): δ 155.6, 146.3, 142.8, 137.5, 131.3 (q, $J = 32.4$ Hz), 128.6, 128.1, 126.7, 126.0 (q, $J = 3.8$ Hz), 124.4 (q, $J = 27.2$ Hz), 120.5 ppm. IR (NaCl): 1327, 1163, 1113, 1087, 1013, 847, 797, 733, 694 cm^{-1} . EI-MS: m/z (M^+) 468, 399.

2,9-Di(4-fluorophenyl)-1,10-phenanthroline (5b). Reaction with tributyl(4-fluorophenyl)stannane (1.64 g, 3.21 mmol) following General procedure 2 and purified by flash chromatography on silica gel (0–20% EtOAc/hexanes) to afford compound **5b** (29 mg, 10% yield) as a colourless amorphous solid. ^1H NMR (400 MHz, CDCl_3): δ 8.46 (dd, $J = 8.8, 5.5$ Hz, 4H), 8.33 (d, $J = 8.4$ Hz, 2H), 8.11 (d, $J = 8.4$ Hz, 2H), 7.81 (s, 2H), 7.30 (m, 4H) ppm. ^{13}C NMR (150 MHz, CDCl_3): δ 164.8, 163.1, 155.8, 146.0, 137.1, 129.5 (d, $J = 8.4$ Hz), 127.7, 126.0, 119.8, 115.8 (d, $J = 21.7$ Hz) ppm. ^{19}F NMR (565 MHz, CDCl_3): δ –112.3 (s, 2F) ppm. IR (NaCl): 1487, 1221, 1157, 932, 907, 838, 722 cm^{-1} . ESI-MS: m/z ($\text{M} + \text{H}^+$) 369.

2,9-Di(3,4-dimethoxyphenyl)-1,10-phenanthroline (5c). Reaction with 3,4-dimethoxyphenylboronic acid (293 mg, 1.61 mmol) following General procedure 1 and purified by flash column chromatography (20–50% EtOAc/hexanes, then 1% MeOH/ CH_2Cl_2) to provide compound **5c** as a colourless amorphous solid (100 mg, 55% yield). ^1H NMR (400 MHz, CDCl_3): δ 8.27–8.23 (complex m, 4H), 8.07 (d, $J = 8.4$ Hz, 2H), 7.94 (d, $J = 8.4$ Hz, 2H), 7.74 (s, 2H), 7.01 (d, $J = 8.4$ Hz, 2H), 4.13 (s, 6H), 3.99 (s, 6H) ppm. ^{13}C NMR (100 MHz, CDCl_3): δ 156.3, 150.8, 149.5, 145.9, 136.9, 132.7, 127.7, 125.7, 120.6, 119.5, 111.5, 111.2, 56.4, 56.1 ppm. IR (NaCl): 1593, 1520, 1489, 1456, 1414, 1273, 1221, 1173, 1157, 1138, 1024, 851, 795, 768, 735, cm^{-1} . EI-MS: m/z (M^+) 452, 437, 421, 405, 377.

2,9-Di(2,4-dimethoxyphenyl)-1,10-phenanthroline (5d). Reaction with 2,4-dimethoxyphenylboronic acid (585 mg, 3.21 mmol) following General procedure 1 and purified by flash column chromatography (30–50% EtOAc/hexanes) to provide compound **5d** as a colourless amorphous solid (113 mg, 31% yield). ^1H NMR (400 MHz, CDCl_3): δ 8.41 (d, $J = 8.5$ Hz, 2H), 8.26 (d, $J = 8.4$ Hz, 2H), 8.20 (d, $J = 8.4$ Hz, 2H), 7.74 (s, 2H), 7.76 (dd, $J = 8.5, 2.3$ Hz, 2H), 6.62 (d, $J = 2.3$ Hz, 2H), 3.914 (s, 6H), 3.911 (s, 6H) ppm. ^{13}C NMR (100 MHz, CDCl_3): δ 161.8, 158.9, 155.8, 146.0, 135.4, 133.4, 127.1, 125.6, 124.4, 122.6, 105.6, 99.0, 55.8, 55.5 ppm. ESI-MS: m/z ($\text{M} + \text{H}^+$) 453.

2,9-Di(4-methoxy-3,5-dimethylphenyl)-1,10-phenanthroline (5e). Reaction with 4-methoxy-3,5-dimethylphenylboronic acid (410 mg, 3.21 mmol) following General procedure 1 and purified by flash column chromatography (1% $\text{NEt}_3/\text{CH}_2\text{Cl}_2$) to provide compound **5e** as a colourless amorphous solid (99 mg, 38% yield). ^1H NMR (400 MHz, CDCl_3): δ 8.28 (d, $J = 8.6$ Hz, 2H), 8.22 (s, 4H), 8.12 (d, $J = 8.12$, 2H), 7.76 (s, 2H), 3.83 (s, 6H), 2.48 (s, 12H) ppm. ^{13}C NMR (100 MHz, CDCl_3): δ 158.7, 156.3, 145.8, 136.9, 134.6, 131.1, 128.3, 127.7, 125.8, 119.6, 59.9, 16.5 ppm. IR (NaCl): 1479, 1321, 1229, 1190, 1165, 1074, 1013, 841, 634 cm^{-1} . EI-MS: m/z (M^+) 448, 433, 418, 403, 388.

2,9-Di(4-methoxy-3,5-di-*tert*-butylphenyl)-1,10-phenanthroline (5f). Reaction with 4-methoxy-3,5-di-*tert*-butylphenylboronic

acid pinacol ester¹³ (556 mg, 1.61 mmol) following General procedure 1 and purified by flash column chromatography on silica gel (EtOAc/hexanes 0–30%) to provide compound **5f** as a colourless amorphous solid (84 mg, 34% yield). This compound is known.¹⁴ ^1H NMR (400 MHz, CDCl_3): δ 8.29 (d, $J = 8.2$ Hz, 2H), 8.13 (s, 4H), 8.03 (d, $J = 8.6$ Hz, 2H), 7.79 (s, 2H), 3.78 (s, 6H), 1.58 (s, 36H) ppm.

2,9-Bis(9,9-dimethyl-9H-fluoren-2-yl)-1,10-phenanthroline (5g). Reaction with (9,9-dimethyl-9H-fluoren-2-yl)boronic acid (500 mg, 2.10 mmol) following General procedure 1 and purified by flash column chromatography on silica gel (0–10% EtOAc/hexanes) to afford compound **5g** (52 mg, 17% yield) as a pale yellow amorphous solid. ^1H NMR (400 MHz, CDCl_3): δ 8.71 (d, $J = 1.2$ Hz, 2H), 8.43 (dd, $J = 7.9, 1.6$ Hz, 2H), 8.35 (d, $J = 8.4$ Hz, 2H), 8.24 (d, $J = 8.4$ Hz, 2H), 7.95 (d, $J = 8.0$ Hz, 2H), 7.88–7.85 (m, 2H), 7.82 (s, 2H), 7.57–7.54 (m, 2H), 7.46–7.39 (complex m, 4H), 1.72 (s, 12H) ppm. ^{13}C NMR (100 MHz, CDCl_3): δ 157.3, 154.6, 154.4, 146.1, 140.8, 138.9, 138.8, 137.1, 128.0, 127.8, 127.2, 127.1, 126.1, 122.8, 122.2, 120.6, 120.5, 120.4, 47.3, 27.5 ppm. IR (NaCl): 1684, 1653, 1584, 1559, 1504, 1447, 1364, 1283, 1225, 1211, 1099, 854, 833, 820, 781, 760, 739 cm^{-1} . ESI-MS: m/z ($\text{M} + \text{H}^+$) 565.

2,9-Bis(4-(9H-carbazol-9-yl)phenyl)-1,10-phenanthroline (5h). Reaction with 9-(4-(tributylstannyl)phenyl)-9H-carbazole¹⁵ (610 mg, 1.15 mmol) following General procedure 2 and purified by flash column chromatography on silica gel (hexanes then CH_2Cl_2) to afford compound **5h** (101 mg, 53% yield) as a pale yellow amorphous solid. ^1H NMR (400 MHz, CDCl_3): δ 8.72 (d, $J = 8.4$ Hz, 4H), 8.45 (d, $J = 8.4$ Hz, 2H), 8.29 (d, $J = 8.4$ Hz, 2H), 8.18 (d, $J = 7.8$ Hz, 4H), 7.91 (s, 2H), 7.84 (d, $J = 8.4$ Hz, 4H), 7.57 (d, $J = 8.2$ Hz, 4H), 7.47 (t, $J = 7.6$ Hz, 4H), 7.33 (t, $J = 7.4$ Hz, 4H) ppm. ^{13}C NMR (100 MHz, CDCl_3): δ 156.3, 146.5, 140.9, 139.0, 138.8, 137.4, 129.4, 128.3, 127.5, 126.4, 126.2, 123.7, 120.5, 120.3, 120.2, 110.1 ppm. IR (NaCl): 1684, 1653, 1559, 1489, 1451, 1362, 750, 723 cm^{-1} . ESI-MS: m/z ($\text{M} + \text{H}^+$) 663.

Preparation of complexes

General procedure 3. These compounds were synthesised by modifying conditions previously reported by Reiser.¹⁶ $[\text{Cu}(\text{CH}_3\text{CN})_4]\text{PF}_6$ (1 equiv.) and the phenanthroline ligand (2 equiv.) were dissolved in CH_2Cl_2 . The ensuing magnetically stirred dark purple solution was maintained at ambient temperature under N_2 . After 2 h, hexanes was added and the precipitated complex was collected by filtration.

Bis(2,9-di(4-(trifluoromethyl)phenyl)-1,10-phenanthroline) copper(i) hexafluorophosphate (3a). Reaction with 2,9-di(4-(trifluoromethyl)phenyl)-1,10-phenanthroline (182 mg, 0.389 mmol) following General procedure 3. Precipitation with hexanes afforded complex **3a** as a dark red solid (218 mg, 97% yield). ^1H NMR (400 MHz, $\text{DMSO}-d_6$): δ 8.86 (d, $J = 8.3$ Hz, 4H), 8.27 (s, 4H), 8.18 (d, $J = 8.3$ Hz, 4H), 7.66 (d, $J = 8.0$ Hz, 8H), 6.92 (d, $J = 8.1$ Hz, 8H) ppm. ^{13}C NMR (150 MHz, $\text{DMSO}-d_6$): δ 154.5, 142.6, 142.0, 138.3, 128.6, 128.5, 126.8, 124.7, 123.88, 123.86, 123.4 (q, $J = 273.3$ Hz) ppm. ESI-MS: m/z 999. HRESIMS [M^+] Found: 999.1390. $\text{C}_{52}\text{H}_{28}\text{CuN}_4\text{F}_{12}$ requires 999.1413.

Bis(2,9-di(4-fluorophenyl)-1,10-phenanthroline)copper(i) hexafluorophosphate (3b). Reaction with 2,9-di(4-fluorophenyl)-1,10-phenanthroline (26 mg, 0.071 mmol) following General procedure 3. Precipitation with hexanes afforded complex **3b** as a dark red solid (32 mg, 97% yield). ^1H NMR (400 MHz, DMSO- d_6): δ 8.65 (d, J = 8.4 Hz, 4H), 8.15 (s, 4H), 7.98 (d, J = 8.3 Hz, 4H), 7.51 (m, 8H), 6.34 (t, J = 8.7 Hz, 8H) ppm. ^{13}C NMR (150 MHz, DMSO- d_6): δ 161.7, 155.5, 143.2, 138.4, 138.4, 135.5 (d, J = 2.6 Hz), 130.3 (d, J = 8.6 Hz), 128.6, 126.9, 125.2, 114.4 (d, J = 21.8 Hz) ppm. HRESIMS [M^+] Found: 799.1522. $\text{C}_{48}\text{H}_{28}\text{CuN}_4\text{F}_4$ requires 799.1541.

Bis(2,9-di(3,4-dimethoxyphenyl)-1,10-phenanthroline)copper(i) hexafluorophosphate (3c). Reaction with 2,9-di(3,4-dimethoxyphenyl)-1,10-phenanthroline (100 mg, 0.222 mmol) following General procedure 3. Precipitation with hexanes afforded complex **3c** as a dark red solid (117 mg, 95% yield). ^1H NMR (400 MHz, DMSO- d_6): δ 8.70 (d, J = 8.0 Hz, 4H), 8.20–8.05 (complex m, 8H), 7.12 (d, J = 7.5 Hz, 4H), 6.96 (s, 4H), 6.03 (d, J = 7.9 Hz, 4H), 3.46 (s, 12H), 3.23 (s, 12H) ppm. ^{13}C NMR (150 MHz, DMSO- d_6): δ 155.7, 149.2, 147.4, 142.9, 137.2, 131.0, 127.5, 125.8, 124.5, 120.2, 110.6, 109.8, 55.1, 54.5 ppm. ESI-MS: m/z 967. HRESIMS [M^+] Found: 967.2738. $\text{C}_{56}\text{H}_{48}\text{CuN}_4\text{O}_8$ requires 967.2763.

Bis(2,9-di(2,4-dimethoxyphenyl)-1,10-phenanthroline)copper(i) hexafluorophosphate (3d). Reaction with 2,9-di(2,4-dimethoxyphenyl)-1,10-phenanthroline (113 mg, 0.250 mmol) following General procedure 3. Precipitation with hexanes afforded complex **3d** as a dark red solid (133 mg, 95% yield). ^1H NMR (400 MHz, DMSO- d_6): δ 8.61 (d, J = 8.3 Hz, 4H), 8.09 (s, 4H), 7.91 (d, J = 8.3 Hz, 4H), 7.08 (d, J = 8.4 Hz, 4H), 5.99 (d, J = 2.2 Hz, 4H), 5.40 (dd, J = 8.4, 2.2 Hz, 4H), 3.46 (s, 12H), 3.44 (s, 12H) ppm. ^{13}C NMR (150 MHz, DMSO- d_6): δ 160.6, 156.7, 154.0, 142.7, 135.7, 129.8, 127.2, 127.0, 125.9, 120.4, 103.1, 96.8, 55.0, 54.7 ppm. HRESIMS [$\text{M} + \text{H}^+$] Found: 967.2763. $\text{C}_{56}\text{H}_{48}\text{CuN}_4\text{O}_8$ requires 967.2768.

Bis(2,9-di(4-methoxy-3,5-dimethylphenyl)-1,10-phenanthroline)copper(i) hexafluorophosphate (3e). Reaction with 2,9-di(4-methoxy-3,5-dimethylphenyl)-1,10-phenanthroline (99 mg, 0.219 mmol) following General procedure 3. Precipitation with hexanes afforded complex **3e** as a dark red solid (89 mg, 73% yield). ^1H NMR (400 MHz, DMSO- d_6): δ 8.75 (d, J = 8.2 Hz, 4H), 8.28 (s, 4H), 8.06 (d, J = 8.2 Hz, 4H), 7.21 (s, 8H), 3.28 (s, 12H), 1.40 (s, 24H) ppm. ^{13}C NMR (100 MHz, DMSO- d_6): δ 157.0, 155.6, 142.7, 137.4, 133.8, 128.9, 128.7, 127.8, 126.4, 124.4, 58.9, 14.9 ppm. HRESIMS [M^+] Found: 959.3583. $\text{C}_{60}\text{H}_{56}\text{CuN}_4\text{O}_4$ requires 959.3592.

Bis(2,9-di(4-methoxy-3,5-di-*tert*-butylphenyl)-1,10-phenanthroline)copper(i) hexafluorophosphate (3f). Reaction with 2,9-di(4-methoxy-3,5-di-*tert*-butylphenyl)-1,10-phenanthroline (115 mg, 0.186 mmol) following General procedure 3, however, this reaction required 7 days to proceed to completion. Precipitation with hexanes afforded known complex **3f** as a dark red solid (105 mg, 78% yield). ^1H NMR (600 MHz, CDCl_3): δ 8.43 (d, J = 8.4 Hz, 4H), 8.04 (s, 4H), 7.85 (d, J = 8.3 Hz, 4H), 7.49 (s, 8H), 3.23 (s, 12H), 0.93 (s, 72H) ppm. ^{13}C NMR (150 MHz, CDCl_3): δ 161.6, 157.2, 143.8, 143.7, 136.4, 133.2, 128.5, 126.7,

125.84, 125.78, 64.6, 35.5, 31.3 ppm. HRESIMS [M^+] Found: 1295.7327. $\text{C}_{84}\text{H}_{104}\text{CuN}_4\text{O}_4$ requires 1295.7348.

Bis(2,9-bis(9,9-dimethyl-9H-fluoren-2-yl)-1,10-phenanthroline)copper(i) hexafluorophosphate (3g). Reaction with 2,9-bis(9,9-dimethyl-9H-fluoren-2-yl)-1,10-phenanthroline (52 mg, 0.087 mmol) following General procedure 3. Precipitation with hexanes afforded complex **3g** as a dark red solid (49 mg, 95% yield). ^1H NMR (400 MHz, DMSO- d_6): δ 8.55 (d, J = 8.4 Hz, 4H), 8.07 (d, J = 8.4 Hz, 4H), 7.96 (s, 4H), 7.89 (s, 4H), 7.57–7.53 (m, 4H), 7.45 (d, J = 7.9 Hz, 4H), 7.43–7.38 (m, 4H), 7.35–7.27 (complex m, 8H), 6.92 (d, J = 7.8 Hz, 4H), 0.93 (s, 24H) ppm. ^{13}C NMR (150 MHz, DMSO- d_6): δ 156.2, 153.3, 152.4, 143.3, 139.3, 137.6, 137.3, 137.2, 128.1, 127.9, 127.2, 127.1, 126.1, 125.3, 122.6, 121.7, 120.3, 118.7, 46.1, 26.1 ppm. ESI-MS: m/z 1191. HRESIMS [M^+] Found: 1191.4412. $\text{C}_{84}\text{H}_{64}\text{CuN}_4$ requires 1191.4422.

Bis(2,9-bis(4-(9H-carbazol-9-yl)phenyl)-1,10-phenanthroline)copper(i) hexafluorophosphate (3h). Reaction with 2,9-bis(4-(9H-carbazol-9-yl)phenyl)-1,10-phenanthroline (100 mg, 0.150 mmol) following General procedure 3. Precipitation with hexanes afforded complex **3h** as a dark red solid (222 mg, 97% yield). ^1H NMR (400 MHz, DMSO- d_6): δ 8.89 (d, J = 8.3 Hz, 4H), 8.36 (d, J = 8.2 Hz, 4H), 8.27–8.19 (complex m, 12 H), 8.01 (d, J = 8.0 Hz, 8H), 7.51 (t, J = 7.5 Hz, 8H), 7.33 (t, J = 7.3 Hz, 8H), 7.04 (d, J = 7.9 Hz, 8H), 6.85 (d, J = 8.0 Hz, 8H) ppm. ^{13}C NMR (150 MHz, DMSO- d_6): δ 155.5, 142.8, 139.3, 138.3, 137.4, 137.2, 129.7, 128.3, 126.7, 126.2, 125.5, 125.0, 122.8, 120.6, 120.4, 109.4 ppm. ESI-MS: m/z 1388. HRESIMS [M^+] Found: 1388.4244. $\text{C}_{84}\text{H}_{64}\text{CuN}_4$ requires 1388.4270.

Photoredox-catalysed reactions

General procedure 4. In a nitrogen filled glovebox, $\text{CF}_3\text{SO}_2\text{Cl}$ (33.9 mg, 200 μmol) was added to a 4 mL screw top vial (PTFE tape-lined thread) containing alkene (100 μmol), K_2HPO_4 (35.1 mg, 200 μmol), copper catalyst (1.0 μmol), CH_3CN (300 μL) and a magnetic stir bar. The vial was then capped, the joint was wrapped with PARAFILM®, and removed from the glovebox and placed in a water bath (suspended with copper wire) maintained at 45 °C that was contained within a 24 W blue LED photoreactor (switched off) and magnetically stirred. The vial was then irradiated. After 24 h, the reaction mixture was quenched by passing through a silica plug (contained within a Pasteur pipette; Et_2O elution) and analysed by ^{19}F NMR spectroscopy (after the addition of PhCF_3 as an internal standard).

3-Chloro-1,1,1-trifluoro-4-methylhexane (13). ^1H NMR (600 MHz, CDCl_3) δ 3.72 (m, 1H), 2.48 (m, 2H), 1.63 (m, 1H), 1.48 (m, 2H), 0.98 (t, J = 7.2 Hz, 3H), 0.90 (s, J = 7.3 Hz, 3H) ppm. ^{19}F NMR (576 MHz, CDCl_3) δ –66.4 (t, J = 14 Hz, 3F) ppm. ^{13}C NMR (150 MHz, CDCl_3) δ 125.8, 63.1, 39.8 (q, J = 31 Hz), 35.6, 27.8, 16.4, 11.8 ppm. HRESIMS [$\text{M} + \text{H}^+$] Found 252.0192. $\text{C}_7\text{H}_{12}\text{ClF}_3\text{O}_2\text{S}$ requires 252.0199.

1,1,1-Trifluoro-4-methylhexane-3-sulfonyl chloride (14). ^1H NMR (600 MHz, CDCl_3) δ 4.13 (m, 1H), 2.05 (m, 2H), 1.94 (m, 1H), 1.54 (quin, J = 4.3 Hz, 2H), 0.93 (s, 3H), 0.89 (s, 3H) ppm. ^{19}F NMR (576 MHz, CDCl_3) δ –66.2 (t, J = 10 Hz, 3F)

ppm. ^{13}C NMR (150 MHz, CDCl_3) δ 123.6, 65.2, 40.3 (q, $J = 26$ Hz), 40.0, 25.9, 19.3, 10.6 ppm. HRESIMS $[\text{M} + \text{H}]^+$ Found 185.0585. $\text{C}_7\text{H}_{12}\text{ClF}_3$ requires 185.0580.

Crystallography

X-ray data were collected at 100 K on crystals mounted on a Hampton Scientific cryoloop on a Bruker AXS D8 Quest diffractometer using $\text{Cu-K}\alpha$ radiation ($\lambda = 1.54178 \text{ \AA}$) or on the MX2 beamlines of the Australian Synchrotron.¹⁸ The structures were solved by direct methods with SHELXT,¹⁹ refined using full matrix least squares routines against F^2 with SHELXL-97 and visualised with OLEX2.²⁰ All non-hydrogen atoms were refined anisotropically. All hydrogen atoms were placed in calculated positions and refined using a riding model with fixed C–H distances of 0.95 \AA ($\text{sp}^2 \text{CH}$), 0.99 \AA (CH_2), 0.98 \AA (CH_3). The thermal parameters of all hydrogen atoms were estimated as $U_{\text{iso}}(\text{H}) = 1.2U_{\text{eq}}(\text{C})$, except for CH_3 where $U_{\text{iso}}(\text{H}) = 1.5U_{\text{eq}}(\text{C})$. The structure of **1-PF₆** has been previously reported at 100 K by Mayer^{5m} and described as containing diffused solvent (two molecules of water in the asymmetric unit, electronic contribution removed with SQUEEZE) when crystallised from a toluene/acetonitrile solvent mixture. Our new report, also at 100 K, appears to be isomorphic (see Results and Discussion section for crystallisation conditions), with the refinement presented in the obtuse triclinic cell setting and containing no solvent accessible voids. We note the cell volume is 12 \AA^3 larger in our case despite the apparent lack of solvent inclusion, with significant improvements in data collection (R_{int}) and refinement metrics presented (R_1 and wR_2). A summary of crystallographic data is provided below, and fully labelled figures are provided in the ESI.†

1-PF₆ (CSD 1872365): $\text{C}_{52}\text{H}_{40}\text{CuF}_6\text{N}_4\text{O}_4\text{P}$, $M = 993.39$, triclinic, $a = 13.7555(4)$, $b = 14.1948(4)$, $c = 14.2099(6)$ \AA , $\alpha = 100.0947(18)^\circ$, $\beta = 118.9449(11)^\circ$, $\gamma = 106.6158(14)^\circ$, $U = 2157.70(14)$ \AA^3 , $T = 100$ K, space group $P\bar{1}$ (no. 2), $Z = 2$, 70597 reflections measured, 7587 unique ($R_{\text{int}} = 0.0434$), $6528 > 4\sigma(F)$, $R = 0.0368$ (observed), $wR_2 = 0.0969$ (all data).

3a (CSD 1872366): $\text{C}_{52}\text{H}_{31}\text{CuF}_{18}\text{N}_5\text{P}$, $M = 1186.35$, monoclinic, $a = 13.3534(7)$, $b = 25.1829(12)$, $c = 13.9516(7)$ \AA , $\beta = 116.8790(10)^\circ$, $U = 4811.5(4)$ \AA^3 , $T = 100$ K, space group $C2/c$ (no. 15), $Z = 4$, 11 427 reflections measured, 2291 unique ($R_{\text{int}} = 0.0330$), $2018 > 4\sigma(F)$, $R = 0.0368$ (observed), $wR_2 = 0.0838$ (all data).

3f (CSD 1872367): $\text{C}_{184}\text{H}_{244}\text{Cu}_2\text{F}_{12}\text{N}_{10}\text{O}_{11}\text{P}_2$, $M = 3188.90$, monoclinic, $a = 43.219(9)$, $b = 15.561(3)$, $c = 26.670(5)$ \AA , $\beta = 102.720(3)^\circ$, $U = 17496(6)$ \AA^3 , $T = 100$ K, space group $P2/c$ (no. 13), $Z = 4$, 156 936 reflections measured, 46 557 unique ($R_{\text{int}} = 0.0548$), $27 444 > 4\sigma(F)$, $R = 0.0721$ (observed), $wR_2 = 0.2416$ (all data).

3g (CSD 1872368): $\text{C}_{86}\text{H}_{67}\text{CuF}_6\text{N}_5\text{P}$, $M = 1378.95$, monoclinic, $a = 24.792(3)$, $b = 18.900(2)$, $c = 15.4325(13)$ \AA , $\beta = 108.117(8)^\circ$, $U = 6872.7(13)$ \AA^3 , $T = 100$ K, space group $C2/c$ (no. 15), $Z = 4$, 21 703 reflections measured, 6032 unique ($R_{\text{int}} = 0.0632$), $4932 > 4\sigma(F)$, $R = 0.0529$ (observed), $wR_2 = 0.1432$ (all data).

Photophysical measurements

Absorption spectra were recorded at room temperature on a PerkinElmer Lambda 35 UV/Vis spectrometer. Uncorrected

steady-state emission and excitation spectra were recorded using an Edinburgh FLSP980-stm spectrometer equipped with a 450 W xenon arc lamp, double excitation and emission monochromators, a Peltier-cooled Hamamatsu R928P photomultiplier (185–850 nm). Emission and excitation spectra were corrected for source intensity (lamp and grating) and emission spectral response (detector and grating) by a calibration curve supplied with the instrument. Emission and excitation spectra were corrected for source intensity (lamp and grating) and emission spectral response (detector and grating) by a calibration curve supplied with the instrument. To record the luminescence spectra at 77 K, the samples were placed in quartz tubes (2 mm diameter) and inserted in a special quartz Dewar filled with liquid nitrogen. Degassing of the dichloromethane solutions was performed using the freeze-pump-thaw method. Experimental uncertainties are estimated to be ± 2 nm and ± 5 nm for absorption and emission peaks, respectively. All the solvents used in the preparation of the solutions for the photophysical investigations were of spectrometric grade.

Electrochemical measurements

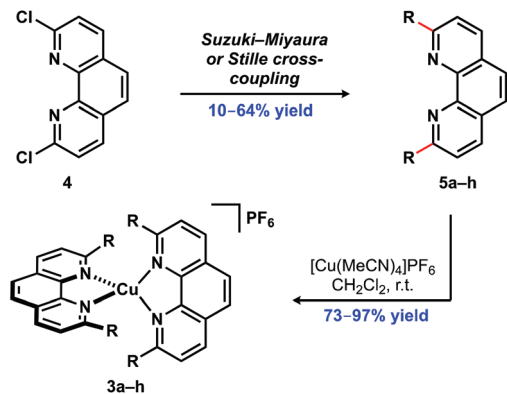
Cyclic voltammetry was performed at room temperature using a Metrohm Autolab PGSTAT101 and data acquired with Metrohm Autolab, Nova 2.0 software. Experiments were performed in dry, degassed CH_3CN (0.25 mM), NBu_4PF_6 (0.1 M) electrolyte, with a CH Instruments glassy carbon working electrode, Pt wire counter electrode, and Ag wire quasi-reference electrode. Ferrocene was added as an internal standard (Fc^+/Fc at 0 V) to reference experiments. The Fc^+/Fc couple has a potential of +0.40 V vs. saturated calomel electrode (SCE) in acetonitrile (NBu_4PF_6 electrolyte).²¹

Results and discussion

Synthesis of ligands and copper(i) complexes

Ligands were prepared using a modular strategy that allowed rapid access to a library of novel phenanthroline derivatives. Key dichloride **4** was synthesised on a multigram scale *via* a previously reported 3-step sequence.²² Palladium-catalysed cross-couplings were then utilised to construct a library of eight 2,9-diaryl-1,10-phenanthrolines **5a–h** (Scheme 2). This approach was adopted as this allowed rapid access to a range of ligands from key intermediate dichloride **4** and commercially available or readily accessible aryl nucleophiles. A common alternative strategy involving lithium-halogen exchange of aryl halides followed by trapping with 1,10-phenanthroline and oxidation with MnO_2 can deliver higher yields for a limited number of related compounds.^{5m,23} However, in our experience, product purification and the reproducibility of this chemistry upon scale-up can be challenging.

The synthesis of homoleptic complexes **3a–h** was achieved by mixing $[\text{Cu}(\text{MeCN})_4]\text{PF}_6$ and the phenanthroline ligand in dichloromethane.¹¹ In this way, a range of electronically- and sterically-varied complexes was prepared. Typically, the for-



Scheme 2 Synthesis of phenanthroline ligands **5a–h** and copper(i) complexes **3a–h**. Reagents and conditions used to synthesise heterocycles **5a–h**: 4 equiv. organoborane, [Pd(PPh₃)₄], Na₂CO₃, 2 : 1 PhMe/H₂O, 95 °C; or 4 equiv. organostannane, [Pd(PPh₃)₄], PhMe, 110 °C.

mation of corresponding bis(phenanthroline)copper(i) complexes **3a–h** was accompanied by the rapid colour change of the reaction mixture (colourless to dark red within 2 h). The conspicuous exception was the synthesis of species **3f**, which proceeded to completion only after 7 days. Armaroli and co-workers made similar observations when they prepared the same complex.¹⁷ In total, eight homoleptic copper(i) species were prepared by this approach, seven of which are previously unreported complexes. The ¹H and ¹³C NMR spectra were obtained for each of the complexes **3a–h**. These spectra are consistent with time-averaged *D*_{2d} symmetric structures in solution in all cases indicating some fluxionality in comparison to the lowered symmetry seen in the solid state. Comparison of the ¹H NMR spectra of the ligands **5a–h** with the respective complexes **3a–h** displays no relative signal broadening or additional signals. This suggests that there is no restricted rotation about the σ-bond connecting the aryl substituents to the phenanthroline moiety in either the free ligands **5a–h** or the complexes **3a–h**.

Solid state structures of complexes **1-PF₆**, **3a**, **3f**, and **3g**

Vapour diffusion of diethyl ether into saturated acetonitrile solutions of complexes **1-PF₆**, **3a**, **3f**, and **3g** provided dark red single crystals suitable for X-ray crystal structure analyses (Fig. 3). Complexes **3a**, and **3g** belong to the monoclinic space group *C*2/*c* and complex **3f** to the monoclinic space group *P*2/*c* while complex **1-PF₆** belongs to the triclinic space group *P*1̄. The asymmetric unit for complex **1-PF₆** comprises a single CuL₂ unit and an anion residue. Both complexes **3a** and **3g** have crystallographic *C*₂ symmetry and contain acetonitrile in the lattice. For **3a**, the acetonitrile molecule is not disordered and the anion residue resides on a crystallographic inversion centre, while for **3g**, the acetonitrile molecule and the anion residue are disordered on a general site with fixed 50% occupancies by virtue of the Cu oxidation state of +1. The asymmetric unit for complex **3f** includes one complete CuL₂ unit and two others residing on crystallographic *C*₂ axes, three

diethyl ether and two acetonitrile solvent molecules and two complete anion residues. The Cu–N bond lengths were typical of related bis(2,9-diarylphenanthroline)copper(i) complexes. For example, Cu–N bond lengths of 2.032(3)–2.112(3) Å have been reported for [bis(2,9-diphenyl-1,10-phenanthroline)copper(i)] tetrafluoroborate (Table 1).²⁴

There is significant distortion from the ideal *D*_{2d} symmetry in each of the complexes **1-PF₆**, **3a**, **3f**, and **3g** consistent with most previously reported bis(phenanthroline)copper(i) species.^{1a,5m,25} The distortions can be defined by three key components; flattening, rocking and wagging distortions (Table 1).^{1a} Flattening distortions were quantified by measuring the interplanar angle between least squares planes of the coordination ring of each ligand. For an ideal tetrahedral metal coordination geometry, the angle would be 90°, which compares to an angle of 0° for an ideal square planar structure. Rocking distortions were quantified by production of a vector between the metal centre and a centroid between C5 and C6 on the phenanthroline backbone of one ligand and measuring the obtuse angles to both nitrogen atoms of the other ligand from this vector. In an ideal tetrahedral metal coordination geometry these angles would be equal. The wagging distortion is a ligand structural feature not directly related to the metal coordination geometry and is defined as the distance between a least squares plane of the phenanthroline backbone of one ligand and the nitrogen atoms of the other ligand. In the absence of wagging these would be equal in absolute value.

Bis(phenanthroline)copper(i) complexes **6a–b** are shown for comparative purposes. Complex **6a** arguably displays the least distortion from an ideal tetrahedral coordination geometry out of the series of 2,9-disubstituted bis(1,10-phenanthroline)copper(i) complexes.²⁶ The steric bulk of the *t*-butyl groups and the absence of π-stacking interactions presumably force the complex to adopt a more ideal tetrahedral geometry and all three flattening, rocking and wagging distortions remain minimal. Conversely, prior to this report, the copper centre within complex **6b** displayed one of the most distorted tetrahedral coordination geometries of the series reported (*vide infra*).²⁷ This potentially stems from enhanced π-stacking interactions as a result of extended conjugation of the 1-naphthyl groups.

Flattening distortions were prevalent in all complexes **1-PF₆**, **3a**, **3f**, and **3g** and likely originate from π-stacking interactions that become available with significant flattening. Furthermore, it has previously been suggested that the flattening distortion derives from more efficient packing in the crystal lattice.²⁵ Complexes containing the [bis(1,10-phenanthroline)copper(i)]⁺ complex ion (**7**) display significant variability in the three key structural distortions described above depending on the counter anion.²⁸ Complex **7-ClO₄** exhibits a pronounced flattening distortion {54.5(5)°} but no rocking or wagging distortion is observed. In contrast, complex **7-CuBr₂** displays only a modest flattening distortion {78.8(3)°} and significant rocking and wagging distortions. However, when comparing complexes **1-PF₆** and **1-BF₄** only small differences in each of the flatten-

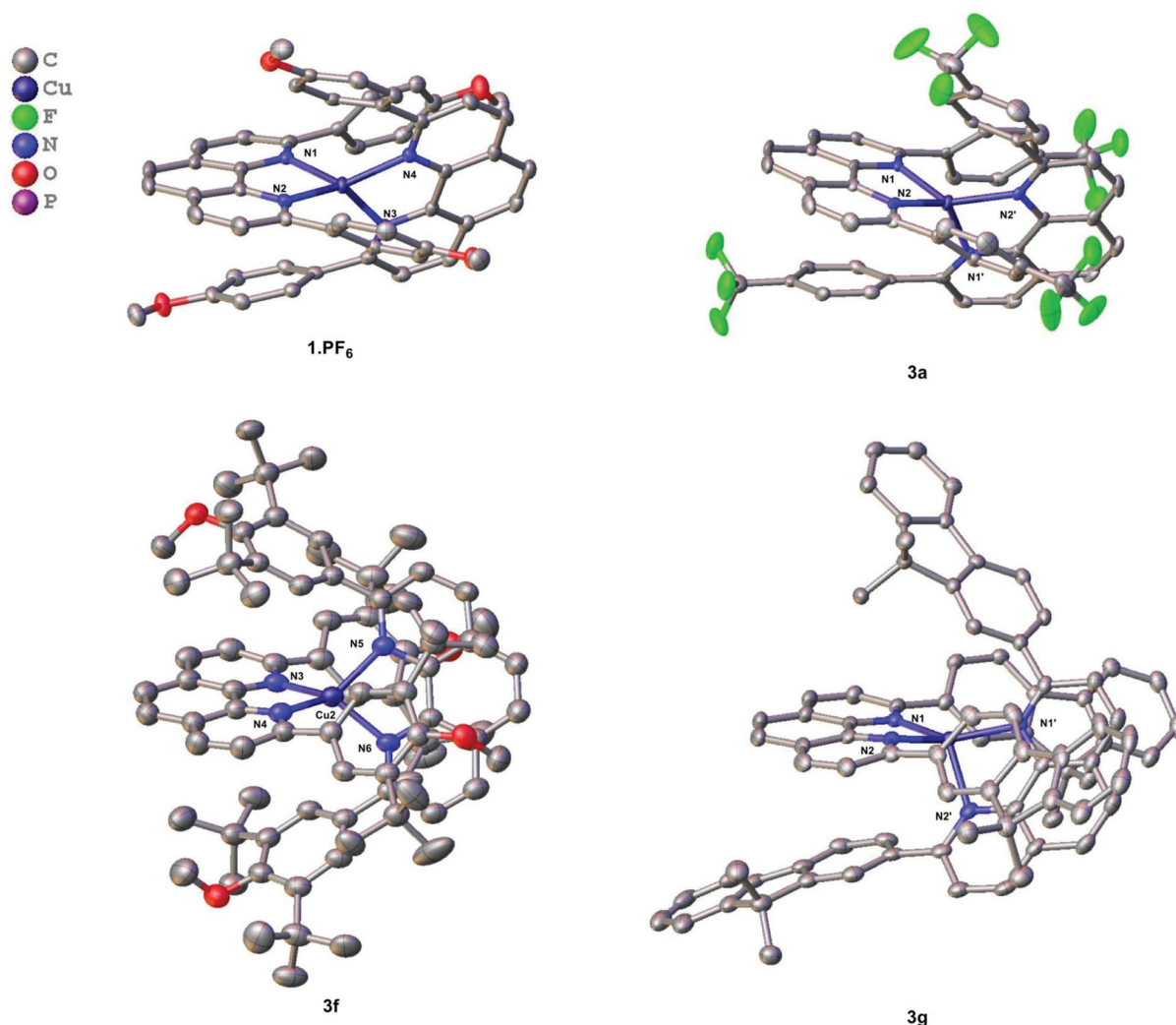


Fig. 3 Structural representations of copper(I) complexes **1-PF₆**, **3a**, **3f**, and **3g**. Thermal ellipsoids are drawn at the 50% probability level. Hexafluorophosphate anions, solvent molecules, hydrogen atoms and disorder have been omitted for clarity (the residue containing a complete CuL₂ unit was chosen to display for complex **3f**). Key bond lengths (Å) and angles (°): **1-PF₆**; Cu–N1 2.045(2), Cu–N2 2.030(2), Cu–N3 2.055(2), Cu–N4 2.027(2), N1–Cu–N2 83.23(8), N3–Cu–N4 83.10(9), **3a** (‘ denotes symmetry operator 1 – x, y, 1/2 – z); Cu–N1 2.055(3), Cu–N2 2.026(3), N1–Cu–N2 83.11(11), **3f**; Cu1–N1 2.028(3), Cu1–N2 2.025(3), Cu2–N3 2.030(2), Cu2–N4 2.022(2), Cu2–N5 2.016(2), Cu2–N6 2.034(2), Cu3–N7 2.015(3), Cu3–N8 2.006(2), N1–Cu1–N2 84.68(18), N3–Cu2–N4 84.63(9), N5–Cu2–N6 84.34(9), N7–Cu3–N8 83.73(13), **3g** (‘ denotes symmetry operator 1 – x, y, 3/2 – z); Cu–N1 2.000(2), Cu–N2 2.112(2), N1–Cu–N2 82.88(8).

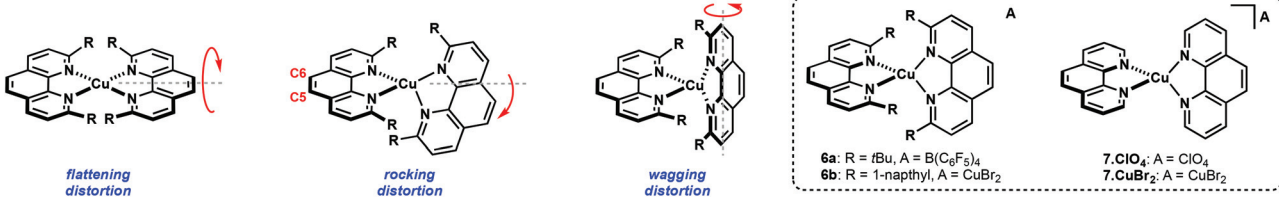
ing, rocking and wagging distortions are observed.²⁹ It is possible that the strong π -stacking interaction, which arises only when 2,9-diaryl substituents are present, increases the effect of intramolecular interactions, such that intermolecular forces do not dominate the influences on the metal coordination geometry and overall structure of the complex ions.

Stronger intramolecular interactions derived from π -stacking may also explain the increased photoexcited state lifetimes observed for several [bis(2,9-diaryl-1,10-phenanthroline)copper(I)]⁺ complexes when compared with related complexes that do not feature 2,9-diaryl substituents. The excited state lifetimes for complex **1-PF₆** (270 ns)^{5a} and [bis(2,9-diphenyl-1,10-phenanthroline)copper(I)] tetrafluoroborate (310 ns)³⁰ which both feature 2,9-diaryl substituents are significantly

increased compared to [bis(2,9-dimethyl-1,10-phenanthroline)copper(I)] chloride (90 ns)³¹ which features 2,9-dimethyl substituents that are incapable of participating in π -stacking. The flattening distortion in complex **3a** is similar to that of complex **1-PF₆** (Table 1). Both of these complexes feature aryl substituents with similar steric bulk (*p*-OMeC₆H₄ and *p*-CF₃C₆H₄). Due to the low steric bulk, both of these substituents allow efficient π -stacking interactions. The flattening distortion was more pronounced in complexes **3f** and **3g**. Whilst this is associated with the increased steric bulk on the 2,9-diaryl substituents the intra- and intermolecular influences are complex.

The rocking distortion for complex **3a** was also similar to that of complex **1-PF₆** and these complexes also exhibit similar

Table 1 Quantification of the distortions within the coordination spheres of complexes **1-PF₆**, **3a**, **3f**, and **3g** and related complexes. The flattening distortion is defined by the interplanar angle between coordination planes for each ligand. The rocking distortion is defined by the angle between a centroid between C5 and C6, the metal centre and the nitrogen atoms on the other ligand. The wagging distortion is defined as the distance between a least squares plane of the phenanthroline backbone of one ligand and the nitrogen atoms of the other ligand. The π -stacking distance refers to the distance between a ring centroid of the aryl substituent on one ligand and the least squares plane of the phenanthroline backbone of the other



[Cu]	Flattening distortion (°)	Rocking distortion (°)	Wagging distortion (Å)	π -Stacking distance (Å)	Cu–N distances (Å)
6a	88.92(5)	136.26(4) & 138.90(3) 133.19(3) & 142.38(4)	–1.322(2) & 1.519(2) –1.076(2) & 1.7371(19)	—	2.096(1)–2.129(1)
6b	73.70 (17)	113.57(13) & 158.59(13) 110.29(13) & 164.29(13)	–0.134(8) & 2.365(6) –0.147(8) & 2.228(7)	3.463(3) & 3.639(3)	2.017(4)–2.120(5)
7-ClO₄	54.4(5)	139.6(2) & 139.6(2) 139.3(2) & 139.3(2)	–1.058(8) & 1.058(8) –1.060 (8) & 1.060(8)	—	2.044(8) & 2.054(8)
7-CuBr₂	78.8(3)	123.9(2) & 149.88(16)	–0.560 (10) & 1.925(9)	—	2.007(8)–2.071(5)
1-PF₆	69.326(2)	119.537(2) & 157.0082(9) 124.569(3) & 150.259(1)	–0.416046(13) & 1.93495(6) –0.80242(3) & 1.61656(6)	3.41379(10) & 3.4001(1)	2.027(2)–2.055(2)
1-BF₄	69.3(4)	121.5(2) & 155.22(18)	–0.495(12) & 1.879(11)	1.396(15)	2.052(6) & 2.067(7)
3a	69.081(4)	119.737(2) & 155.445(1)	–0.61598(2) & 1.76772(7)	3.3836(1)	2.026(3) & 2.055(3)
3f	63.551(11)–66.94(3)	137.659(8) & 137.659(8) 137.770(8) & 137.770(8) 135.883(16) & 139.374(8) 137.43(2) & 138.198(11) 137.211(8) & 137.211(8) 138.134(11) & 138.134(11)	–1.1938(4) & 1.1938(4) –1.1819(3) & 1.1819(3) –1.0427(2) & 1.3268(3) –1.15031(18) & 1.20839(18) –1.2199(3) & 1.2199(3) –1.2150(3) & 1.2150(3)	3.5862(6)–3.8021(9)	2.0066(4)–2.0337(4)
3g	64.195(8)	109.364(7) & 162.497(3)	–0.150878(11) & 2.00949(14)	3.5378(3)	2.0000(2) & 2.112(2)

6a: R = *t*Bu, A = B(C₆F₅)₄
 6b: R = 1-naphthyl, A = CuBr₂
 7: ClO₄, A = ClO₄
 7: CuBr₂, A = CuBr₂

π -stacking distances to each other (Table 1). In contrast, the rocking distortion is increased in complex **3g**. The *gem*-dimethyl groups present in complex **3g** provide an increase in the π -stacking distance, however, a more pronounced rocking distortion is observed. The rocking distortion in complex **3f** is significantly reduced and a longer π -stacking distance is observed. Potentially, the greater steric bulk, particularly of the *m*-(*t*-Bu) groups and the symmetrical distribution of the bulk almost completely prevents the rocking distortion in **3f**.

Wagging distortions follow a similar trend with the extent of the distortion for complex **3a** remaining similar to that of complex **1-PF₆** and complex **3f** displays more limited distortion. This potentially derives from the steric parameters of the respective aryl substituents. Interestingly, complex **3g** features the most significant distortion. This potentially originates from the unsymmetrical steric bulk of the 2,9-diaryl substituents with the orientation of the *gem*-dimethyl group forcing a more significant wagging distortion.

Armaroli and co-workers previously reported complex **3f** and demonstrated its kinetic inertness to ligand dissociation.¹⁷ These researchers demonstrated that the complex was inert to ligand exchange even in the presence of excess 1,10-phenanthroline, over extended time frames and at reflux in dichloromethane or acetonitrile despite the lack of steric bulk in unsubstituted 1,10-phenanthroline. This contrasts

with related homoleptic bis(phenanthroline)copper(I) complexes that feature less bulkier ligands than phenanthroline **5f**. Such complexes typically participate in ligand substitution reactions in the presence of even less bulky 1,10-phenanthroline-based ligands according to the HETPHEN (heteroleptic bisphenanthroline complexes) principle.³² Armaroli and co-workers also reported extended timeframes for the synthesis of complex **3f** and suggested that these observations derive from the steric bulk of the ligand, however, the solid state structure was not reported in their study. Notably, the solid state structure reported here suggests that the bulk of the 2,9-diaryl substituents in complex **3f** may be responsible for the kinetic locking of the ligands within the complex. The high steric congestion in this complex **3f**, discussed above, supports this.

Photophysical studies

Selected photophysical data are reported in Table 2. The absorption spectra of the homoleptic copper(I) complexes, measured from diluted dichloromethane solutions, were typically quite similar and with most complexes exhibiting strong absorption bands between 250–400 nm, which are attributed to ligand centred (LC) π - π^* transitions (Fig. 4 and ESI†). The complexes also exhibited broad absorption bands of weaker intensity between 420–600 nm. These respective bands are attributed to excitation to the MLCT manifold.¹ In each case,

Table 2 Electronic absorption and luminescence data for copper-complexes **1-PF₆**, and **3a–h**. Measurements were performed in CH₂Cl₂ at 298 K unless otherwise noted

[Cu]	Absorption		Excitation	Emission	
	λ_{\max} (nm)	$10^4 \epsilon$ (M ⁻¹ cm ⁻¹)	λ_{exc} (nm)	λ_{\max}^b deaerated (nm)	λ_{\max}^a (nm)
1-PF₆	443	0.404	440	550 _{sh} , 716	—
	577	0.235			
3a	436	0.411	430	705	750
	563	0.203			
3b	439	0.388	400	720	760
	567	0.159			
3c	453	0.347	430	530, 715 _{sh}	590
	587	0.133			
3d	473	0.323	430	580	750
3e	450	0.517	400	750	785
	571	0.372			
3f	451	0.483	400	640	820
	574	0.417			
3g	524	0.295	430	630	760
3h	560	0.127	430	535, 715 _{sh}	560

^a Measurements were performed at 77 K. ^b The shoulder in the emission spectrum is reported as “sh”

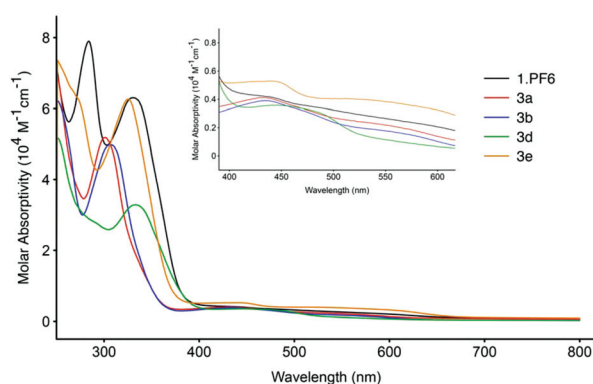


Fig. 4 Absorption spectra of selected homoleptic copper(I) complexes performed in CH₂Cl₂.

these broad absorption bands fall within the visible spectrum and shows that these complexes can be excited by irradiating with visible light for the purpose of photocatalysis.^{5a}

Upon excitation to the MLCT manifold, the complexes are poorly emissive in degassed dichloromethane solutions at room temperature (see ESI†). For some complexes, a band of weak intensity is visible between 600 and 800 nm, which is mainly ascribed to emission from singlet ¹MLCT as a result of thermally activated delayed fluorescence (TADF) commonly observed for copper(I) complexes.³³

Electrochemical studies

The oxidation potential of the M^I/M^{II} couple was measured directly by cyclic voltammetry for copper(I) complexes **3** (and compound **1-PF₆**). The majority of the synthesised copper(I) complexes maintained reversible behaviour for the M^I/M^{II} couple similar to that of the parent [Cu(dap)₂]PF₆ (**1-PF₆**)

Table 3 Electrochemical data for copper complexes **1-PF₆** and **3a–h** in degassed CH₃CN at ambient temperature. All potentials are given in volts (V) versus the saturated calomel electrode (SCE)

	[Cu]	$E_{1/2}$ (M ^I /M ^{II})
1	1-PF₆	+0.62
2	3a	+0.89
3	3b	+0.78
4	3c	+0.68
5	3d	+0.51
6	3e	+0.66
7	3f	+0.69
8	3g	+0.68
9	3h	+0.79

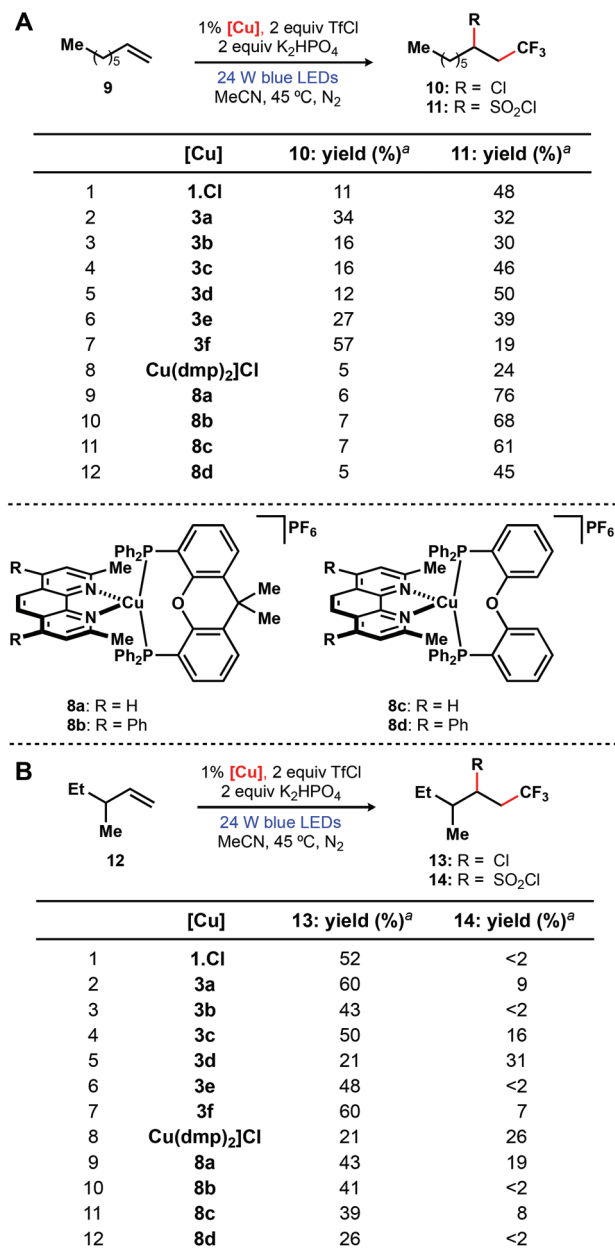
($E_{1/2}^{I/II} = +0.62$ V vs. SCE) (Table 3). However, there were several notable deviations. Both complexes **3a** and **3b**, featuring 2,9-diarylphenanthroline ligands containing *p*-electron-withdrawing substituents, featured higher oxidation potentials than parent complex **1-PF₆**. Molecules **3c**, **3e**, **3f**, and **3g**, which contain electron-donating aryl substituents, maintained oxidation potentials similar to [Cu(dap)₂]PF₆ (**1-PF₆**). In contrast, complex **3d**, which features *o,p*-dimethoxy-aryl groups, displayed a lower oxidation potential ($E_{1/2}^{I/II} = +0.51$ V vs. SCE), while molecule **3h** containing a carbazole moiety featured a higher oxidation potential ($E_{1/2}^{I/II} = +0.79$ V vs. SCE).

On the basis of the photophysical data obtained for copper complexes **3**, we did not determine the excited state redox potentials of these complexes.³⁴

Photoredox catalysis

In 2015, Reiser and co-workers reported a photoredox-catalysed ATRA reaction facilitated by [Cu(dap)₂]Cl (**1-Cl**) that provided notable divergent reactivity in comparison to [Ru(bpy)₃]Cl₂ (**2**) (Scheme 1).^{5f} The authors postulated that in addition to serving as a classical photoredox catalyst, the copper complex coordinates reactive intermediates derived from triflyl chloride and, thus, is also involved in key-bond forming steps leading to the formation of the chlorosulfonylation product. Consistent with this postulate, these researchers also observed that increasing steric bulk, both with respect to the copper photoredox catalyst and the olefin substrate, disfavours the chlorosulfonylation process relative to the chlorination pathway.^{5f} Consequently, we aimed to utilise this intriguing reaction to indirectly investigate the influence of various structural and other fundamental properties of copper(I) complexes **3a–f** on the outcomes of such ATRA processes. In order to complete a more extensive study, [Cu(dap)₂]Cl (**1-Cl**), [Cu(dmp)₂]Cl, and known heteroleptic copper(I) complexes **8a–d** were also included in this work (Scheme 3).³⁵

First, we investigated the copper-photoredox-catalysed reaction of triflyl chloride with 1-octene (**9**) (Scheme 3A). All of the complexes that were screened promoted a reaction, and in the majority of cases these reactions proceeded to complete conversion.^{36–38} [Cu(dap)₂]Cl (**1-Cl**) provided a ~4 : 1 ratio of compounds **11** and **10**. Interestingly, the essentially isosteric complexes **3a** and **3b**, which both feature ligands containing



Scheme 3 (A) Outcomes of copper(I) photoredox-catalysed ATRA reactions featuring 1-octene (9). (B) Outcomes of copper(I) photoredox-catalysed ATRA reactions featuring sterically hindered 3-methyl-1-pentene (12). dmp = 2,9-dimethyl-1,10-phenanthroline. ^a Yields determined by ¹⁹F NMR spectroscopy with the aid of a calibrated internal standard (average of 2 experiments).

p-electron-withdrawing aryl substituents afforded ~1:1 and ~2:1 ratios of chlorosulfonylation/chlorination products, respectively. Importantly, these data suggest that electronic factors may also play a significant role in controlling the viability of the chlorosulfonylation pathway in this chemistry. Bulkier catalysts **3c** and **3d**, which feature ligands containing *m,p*-(OMe)₂- and *o,p*-(OMe)₂-substituted aryl moieties, furnished ~3:1 and ~4:1 ratios of compounds **11** and **10**, respectively. In contrast, the more sterically encumbered species **3e**

and **3f** afforded ~1.5:1 and ~1:3 ratios of chlorosulfonylation/chlorination products, respectively. [Cu(dmp)₂]Cl and heteroleptic copper(I) catalysts **8a–d**, which are less bulky than [Cu(dap)₂]Cl, provided these chlorosulfonylation/chlorination products in generally much higher ratios (~5:1 to ~13:1).

Next, 3-methyl-1-pentene (**12**) was employed as a substrate and, consistent with our expectations, employing this more sterically hindered olefin significantly biased these transformations to heavily favour the chlorination pathway (Scheme 3B). Specifically, homoleptic copper(I) catalysts **1.Cl**, **3b**, **3e** furnished chlorination product **13** essentially exclusively, while complexes **3a**, **3c**, and **3f** afforded ~1:7, and ~1:3, ~1:9 ratios of chlorosulfonylation/chlorination products, respectively. Interestingly, photoredox-catalyst **3d** facilitated a ~1.5:1 ratio of compounds **14** and **13**. The reasons for this are unclear. Although [Cu(dmp)₂]Cl enabled the synthesis of compounds **14** and **13** in a ~1:1 ratio, heteroleptic copper(I) catalysts **8a–d** particularly favoured the formation of chloride **13**.

The ability of several members of this class of copper-based complexes to catalyse this ATRA reaction showcases the utility of these complexes as photoredox catalysts. The simple variation of the steric and electronic parameters of the copper complexes has a pronounced effect on the outcome of the reaction. This demonstrates the potential of these complexes for catalyst screening purposes in other photoredox-catalysed processes, particularly those in which inner-sphere reactivity is invoked.

Conclusions

We have synthesised a range of previously unreported homoleptic 2,9-diaryl-1,10-phenanthroline copper(I) complexes (**3a–h**). These complexes were spectroscopically characterised and the solid state structures of three of these compounds were determined by single-crystal X-ray analysis. The quantification of the distortion away from an ideal tetrahedral coordination geometry suggests that the 2,9-diaryl substituents play a significant role in the overall structure of the complex. Structure **3g** displayed the most significant distortion. In addition, our results suggest that the reported kinetic locking of the ligands within complex **3f** is consistent with the high steric congestion observed in the solid state.¹⁷ The modular approach employed for ligand synthesis allows access to a range of electronically- and sterically-varied complexes.

The complexes can be photoexcited with visible light to their MLCT manifold, thus allowing photocatalysed reactions activated by visible light. These homoleptic copper(I) species, and various known heteroleptic copper(I) complexes, were also evaluated in order to determine their capacity to promote ATRA processes leading to trifluoromethylchlorosulfonylation and trifluoromethylchlorination products. The outcomes of these photoredox-catalysed reactions were generally consistent with the varying steric bulk of the copper complex employed. However, our results reveal that electronic factors may also play a significant role in controlling the viability of the chlorosulfonylation pathway in this chemistry.

Conflicts of interest

There are no conflicts to declare.

Acknowledgements

We gratefully acknowledge the University of Tasmania, School of Natural Sciences – Chemistry, ATA Scientific (T.P.N.), RACI (T.P.N.), and the Collier Charitable Fund (A.C.B.) for financial support and PhosAgro/UNESCO/IUPAC for a Green Chemistry for Life Grant (A.C.B.). T.P.N. thanks the Australian Government for a Research Training Program Scholarship. We thank the University of Tasmania Central Science Laboratory for providing access to NMR spectroscopy services. This research was undertaken, in part, using the MX2 beamline at the Australian Synchrotron, part of ANSTO, and made use of the Australian Cancer Research Foundation (ACRF) detector. We thank reviewers for helpful comments.

Notes and references

- For selected reviews on the fundamental properties of bis (1,10-phenanthroline)copper(i) complexes and their applications in visible-light-mediated photoredox catalysis, see: (a) N. Armaroli, *Chem. Soc. Rev.*, 2001, **30**, 113–124; (b) N. Armaroli, G. Accorsi, F. Cardinali and A. Listorti, *Photochemistry and Photophysics of Coordination Compounds: Copper*, in *Topics in Current Chemistry* 280, ed. V. Balzani and S. Campagna, Springer, Berlin, Germany, 2007, pp. 69–116; (c) A. Lavie-Cambot, M. Cantuel, Y. Leydet, G. Jonusauskas, D. M. Bassani and N. D. McClenaghan, *Coord. Chem. Rev.*, 2008, **252**, 2572–2584; (d) S. Paria and O. Reiser, *ChemCatChem*, 2014, **6**, 2477–2483; (e) A. C. Hernandez-Perez and S. K. Collins, *Acc. Chem. Res.*, 2016, **49**, 1557–1565; (f) O. Reiser, *Acc. Chem. Res.*, 2016, **49**, 1990–1996; (g) A. Olding, T. P. Nicholls and A. C. Bissember, *Aust. J. Chem.*, 2018, **71**, 547–548.
- See, for example: M. Geoffroy, M. Wermeille, C. O. Buchecker, J.-P. Sauvage and G. Bernardinelli, *Inorg. Chim. Acta*, 1990, **167**, 157–164.
- M. Miller, P. K. Gantzel and T. B. Karpishin, *Inorg. Chem.*, 1998, **37**, 2285–2290.
- For selected recent reviews on visible-light-mediated photoredox catalysis, see: (a) C. K. Prier, D. A. Rankic and D. W. C. MacMillan, *Chem. Rev.*, 2013, **113**, 5322–5363; (b) T. Koike and M. Akita, *Synlett*, 2013, **24**, 2492–2505; (c) T. P. Nicholls, D. Leonori and A. C. Bissember, *Nat. Prod. Rep.*, 2016, **33**, 1248–1254; (d) M. H. Shaw, J. Twilton and D. W. C. MacMillan, *J. Org. Chem.*, 2016, **81**, 6898–6926; (e) L. Marzo, S. K. Pagire, O. Reiser and B. König, *Angew. Chem., Int. Ed.*, 2018, **57**, 10034–10072.
- For examples of synthetic processes utilizing homoleptic Cu(i) phenanthroline-based visible-light-mediated photoredox catalysts, see: (a) J.-M. Kern and J.-P. Sauvage, *J. Chem. Soc., Chem. Commun.*, 1987, 546–548; (b) M. Pirtsch, S. Paria, T. Matsuno, H. Isobe and O. Reiser, *Chem. – Eur. J.*, 2012, **18**, 7336–7340; (c) A. Baralle, L. Fensterbank, J.-P. Goddard and C. Ollivier, *Chem. – Eur. J.*, 2013, **19**, 10809–10813; (d) S. Paria, M. Pirtsch, V. Kais and O. Reiser, *Synthesis*, 2013, **45**, 2689–2698; (e) X.-J. Tang and W. R. Dolbier, *Angew. Chem., Int. Ed.*, 2015, **54**, 4246–4249; (f) D. B. Bagal, G. Kachkovskiy, M. Knorn, T. Rawner, B. M. Bhanage and O. Reiser, *Angew. Chem., Int. Ed.*, 2015, **54**, 6999–7002; (g) G. Fumagalli, P. T. G. Rabet, S. Boyd and M. F. Greaney, *Angew. Chem., Int. Ed.*, 2015, **54**, 11481–11484; (h) Z. Zhang, X. Tang, C. S. Thomason and W. R. Dolbier, *Org. Lett.*, 2015, **17**, 3528–3531; (i) T. P. Nicholls, G. C. Constable, J. C. Robertson, M. G. Gardiner and A. C. Bissember, *ACS Catal.*, 2016, **6**, 451–457; (j) P. T. G. Rabet, G. Fumagalli, S. Boyd and M. F. Greaney, *Org. Lett.*, 2016, **18**, 1646–1649; (k) T. Rawner, M. Knorn, E. Lutsker, A. Hossain and O. Reiser, *J. Org. Chem.*, 2016, **81**, 7139–7147; (l) S. K. Pagire, S. Paria and O. Reiser, *Org. Lett.*, 2016, **18**, 2106–2109; (m) M. M. Cetin, R. T. Hodson, C. R. Hart, D. B. Cordes, M. Findlater, D. J. Cassadonte Jr., A. F. Cozzolino and M. F. Mayer, *Dalton Trans.*, 2017, **46**, 6553–6569; (n) T. Rawner, E. Lutsker, C. A. Kaiser and O. Reiser, *ACS Catal.*, 2018, **8**, 3950–3956; (o) A. Hossain, A. Vidyasagar, C. Eichinger, C. Lankes, J. Phan, J. Rehbein and O. Reiser, *Angew. Chem., Int. Ed.*, 2018, **57**, 8288–8292.
- For examples of synthetic processes utilising heteroleptic Cu(i) phenanthroline-based visible-light-mediated photoredox catalysts, see: (a) A. C. Hernandez-Perez, A. Vlassova and S. K. Collins, *Org. Lett.*, 2012, **14**, 2988–2991; (b) A. C. Hernandez-Perez and S. K. Collins, *Angew. Chem., Int. Ed.*, 2013, **52**, 12696–12700; (c) M. Knorn, T. Rawner, R. Czerwieniec and O. Reiser, *ACS Catal.*, 2015, **5**, 5186–5193; (d) A. C. Hernandez-Perez, A. Caron and S. K. Collins, *Chem. – Eur. J.*, 2015, **21**, 16673–16678; (e) A. Call, C. Casadevall, F. Acuña-Parés, A. Casitas and J. Lloret-Fillol, *Chem. Sci.*, 2017, **8**, 4739–4749; (f) B. Michelet, C. Deldaele, S. Kajou, C. Moucheron and G. Evano, *Org. Lett.*, 2017, **19**, 3576–3579; (g) W. Zhao, R. P. Wurz, J. C. Peters and G. C. Fu, *J. Am. Chem. Soc.*, 2017, **139**, 12153–12156; (h) T. P. Nicholls, J. C. Robertson, M. G. Gardiner and A. C. Bissember, *Chem. Commun.*, 2018, **54**, 4589–4592; (i) C. Minozzi, A. Caron, J.-C. Grenier-Petel, J. Santandrea and S. K. Collins, *Angew. Chem., Int. Ed.*, 2018, **57**, 5477–5481; (j) H. Baguia, C. Deldaele, E. Romero, B. Michelet and G. Evano, *Synthesis*, 2018, **50**, 3022–3030.
- For examples of studies investigating the various structural, photophysical, and electrochemical properties of homoleptic 2,9-diaryl-1,10-phenanthroline copper(i) complexes published since 2008, see: ref. 5m; (a) M. Iwamura, F. Kobayashi and K. Nozaki, *Chem. Lett.*, 2016, **45**, 167–169; (b) G. Capano, U. Rothlisberger, I. Tavernelli and T. J. Penfold, *J. Phys. Chem. A*, 2015, **119**, 7026–7037; (c) M. Iwamura, S. Takeuchi and T. Tahara, *Acc. Chem. Res.*, 2015, **48**, 782–791; (d) L. Hua, M. Iwamura, S. Takeuchi and

- T. Tahara, *Phys. Chem. Chem. Phys.*, 2015, **17**, 2067–2077; (e) M. Iwamura, S. Takeuchi and T. Tahara, *Phys. Chem. Chem. Phys.*, 2014, **16**, 4143–4145; (f) C. E. McKusker and F. N. Castellano, *Chem. Commun.*, 2013, **49**, 3537–3539; (g) M. W. Mara, N. E. Jackson, J. Huang, A. B. Stickrath, X. Zhang, N. A. Gothard, M. A. Ratner and L. X. Chen, *J. Phys. Chem. B*, 2013, **117**, 1921–1931; (h) L.-Y. Zou, M.-S. Ma, Z.-L. Zhang, H. Li, Y.-X. Cheng and A.-M. Ren, *Org. Electron.*, 2012, **13**, 2627–2638; (i) P. Yang, X.-J. Yang and B. Wu, *Eur. J. Inorg. Chem.*, 2009, 2951–2958. For detailed reviews of research in this area prior to 2008, see ref. 1a–c.
- 8 H. C. Guo, H. Zheng and H. J. Jiang, *Org. Prep. Proced. Int.*, 2012, **44**, 392–396.
 - 9 D. R. McMillin, M. T. Buckner and B. T. Ahn, *Inorg. Chem.*, 1977, **16**, 943–945.
 - 10 (a) S.-P. Luo, E. Mejía, A. Friedrich, A. Pazidis, H. Junge, A.-E. Surkus, R. Jackstell, S. Denurra, S. Gladiali, S. Lochbrunner and M. Beller, *Angew. Chem., Int. Ed.*, 2013, **52**, 419–423; (b) M. Heberle, S. Tschierlei, N. Rockstroh, M. Ringenberg, W. Frey, H. Junge, M. Beller, S. Lochbrunner and M. Karnahl, *Chem. – Eur. J.*, 2017, **23**, 312–319.
 - 11 J. Frey, T. Kraus, V. Heitz and J.-P. Sauvage, *Chem. – Eur. J.*, 2007, **13**, 7584–7594.
 - 12 D. Milstein and J. K. Stille, *J. Am. Chem. Soc.*, 1979, **101**, 4992–4998.
 - 13 V. Diemer, H. Chaumeil, A. Defoin, A. Fort, A. Boeglin and C. Carré, *Eur. J. Org. Chem.*, 2008, 1767–1776.
 - 14 A. J. Pallenberg, K. S. Koenig and D. M. Barnhart, *Inorg. Chem.*, 1995, **34**, 2833–2840.
 - 15 V. Koch, M. Nieger and S. Bräse, *Adv. Synth. Catal.*, 2017, **359**, 832–840.
 - 16 M. Pirtsch, S. Paria, T. Matsuno, H. Isobe and O. Reiser, *Chem. – Eur. J.*, 2012, **18**, 7336–7340.
 - 17 V. Kalsani, M. Schmittel, A. Listorti, G. Accorsi and N. Armaroli, *Inorg. Chem.*, 2006, **45**, 2061–2067.
 - 18 T. M. McPhillips, S. E. McPhillips, H. J. Chiu, A. E. Cohen, A. M. Deacon, P. J. Ellis, E. Garman, A. Gonzalez, N. K. Sauter, R. P. Phizackerley, S. M. Soltis and P. Kuhn, *J. Synchrotron Radiat.*, 2002, **9**, 401–406.
 - 19 G. M. Sheldrick, *Acta Crystallogr.*, 2015, **71**, 3–8.
 - 20 O. V. Dolomanov, L. J. Bourhis, R. J. Gildea, J. A. K. Howard and H. Puschmann, *J. Appl. Crystallogr.*, 2009, **42**, 339–341.
 - 21 N. G. Connelly and W. E. Geiger, *Chem. Rev.*, 1996, **96**, 877–910.
 - 22 H. C. Guo, R. H. Zheng and H. J. Jiang, *Org. Prep. Proced. Int.*, 2012, **44**, 392–396.
 - 23 (a) C. Dietrich-Buchecker and J.-P. Sauvage, *Tetrahedron*, 1990, **46**, 503–512; (b) S. Kang, M. M. Cetin, R. Jiang, E. S. Clevenger and M. F. Mayer, *J. Am. Chem. Soc.*, 1014, **136**, 12588–12591.
 - 24 M. T. Miller, P. K. Gantzel and T. B. Karpishin, *Inorg. Chem.*, 1998, **37**, 2285–2290.
 - 25 J. E. Beves, B. A. Blight, C. J. Campbell, D. A. Leigh and R. T. McBurney, *Angew. Chem., Int. Ed.*, 2011, **50**, 9260–9327.
 - 26 B. A. Gandhi, O. Green and J. N. Burstyn, *Inorg. Chem.*, 2007, **46**, 3816–3825.
 - 27 P. Yang, X.-J. Yang and B. Wu, *Eur. J. Inorg. Chem.*, 2009, 2951–2958.
 - 28 P. C. Healy, L. M. Engelhardt, V. A. Patrick and A. H. White, *J. Chem. Soc., Dalton Trans.*, 1985, 2541–2545.
 - 29 M. Geoffroy, M. Wermeille, C. O. Buchecker, J.-P. Sauvage and G. Bernardinelli, *Inorg. Chim. Acta*, 1990, **167**, 157–164.
 - 30 C. O. Dietrich-Buchecker, P. A. Marnot, J.-P. Sauvage, J. R. Kirchhoff and D. R. McMillin, *J. Chem. Soc., Chem. Commun.*, 1983, 513–515.
 - 31 J. R. Kirchhoff, R. E. Gamache Jr., M. W. Blaskie, A. A. Del Paggio, R. K. Lengel and D. R. McMillin, *Inorg. Chem.*, 1983, **22**, 2380–2384.
 - 32 (a) V. Kalsani, H. Bodenstedt, D. Fenske and M. Schmittel, *Eur. J. Inorg. Chem.*, 2005, 1841–1849; (b) R. Colton, B. D. James, I. D. Potter and J. C. Traeger, *Inorg. Chem.*, 1993, **32**, 2626–2629.
 - 33 For examples of studies of copper(i) complexes featuring TADF, see: (a) K.-C. Chan, S.-C. Cheng, L. T.-L. Lo, S.-M. Yiu and C.-C. Ko, *Eur. J. Inorg. Chem.*, 2018, 897–903; (b) L. Lv, K. Yuan and Y. Wang, *Phys. Chem. Chem. Phys.*, 2018, **20**, 6548–6561; (c) L. Lin, D.-H. Chen, R. Yu, X.-L. Chen, W.-J. Zhu, D. Liang, J.-F. Chang, Q. Zhang and C.-Z. Lu, *J. Mater. Chem. C*, 2017, **5**, 4495–4504.
 - 34 J. R. Lakowicz, *Principles of Fluorescence Spectroscopy*, Springer, USA, 3rd edn, 2010.
 - 35 The reported electrochemical data for Cu(dmp)₂]PF₆ and copper complexes **8a–d** is provided in the ESI.†
 - 36 A series of control experiments determined that no reaction occurs in the absence of light and that no reaction occurs in the absence of the copper complexes.
 - 37 When the reaction shown in Scheme 3A was performed in the presence of 2 equiv. TEMPO (a radical trap) essentially no reaction occurred.
 - 38 CD₃CN solutions of the copper complexes were irradiated for 24 h. In each case, no changes in the respective ¹H NMR spectra associated with these complexes could be identified.